

Implementation of Robust Feedback Linearization on Active Magnetic Bearing Actuators

Min Chen and Carl R. Knospe

Department of Mechanical and Aerospace Engineering, University of Virginia, Charlottesville, VA 22903
crk4y@virginia.edu

ABSTRACT

Feedback linearization is a promising approach to solve the nonlinear control problem for active magnetic bearing systems. In this paper, feedback linearization is employed in combination with robust control techniques for the regulation of a machine tool system actuated by a magnetic bearing. A nonlinear, high order polynomial model was developed based on experimental calibration of the magnetic bearing. The effect of the amplifier and sensor dynamics on the feedback linearization performance was also determined and compensated. Finally, an uncertainty framework was proposed for the linearized plant and a robust controller was designed via μ synthesis. Experimental results show that the feedback-linearized active magnetic bearing system can achieve both high performance as well as stability over the entire bearing clearance.

1 INTRODUCTION

Active Magnetic Bearings (AMBs) have been of increasing interest to the manufacturing industry, due to their high force capacity, relatively large travel range, high speed capability, and potential for high damping via active control. However, AMB systems are highly nonlinear and open loop unstable. Thus, when high performance is desired, they present an extremely challenging control problem. In recent years, feedback linearization approach has been widely discussed in AMB applications [1, 3, 4, 5]. This approach utilizes a complete nonlinear description of an AMB system to yield a feedback law that transforms the plant to a linear one. Therefore, feedback linearized AMB systems should behave linearly over a much larger travel range than achievable using traditional Jacobian linearization [7].

Feedback linearization approach has been widely implemented in simple magnetic levitation systems consisting of one or two electromagnets [1, 3, 5]. However, for typically-used multiple-pole ra-

dial magnetic bearings, most investigations have focused on theoretical analysis and computer simulation [8, 9]. Few experimental results have been reported in the literature. One reason for this situation is the difficulty of developing simple yet accurate multiple-pole AMB models, which have a significant influence on the success of feedback linearization approach.

Feedback linearization transforms the original nonlinear system into a linear one through exact cancellation of system nonlinearities. In practice, this cancellation will not be perfect due to the uncertainty in bearing models (e.g. variations in coil resistance due to changes in bearing temperature [3]). In this paper, we propose an uncertainty structure for the linearized plant nominal model. This uncertainty description can be validated from experimental results. As a consequence, the feedback linearization approach can be combined with linear robust control techniques to guarantee the nonlinear system stability and performance in the presence of model uncertainty and disturbances.

For our experiment, we employ a single axis machine tool system driven by an AMB actuator. Due to the large cutting force in machining process, and the compliance of the structure, the bearing journal must be capable of large travel within the clearance. Feedback linearization is applied on this system. We will focus our discussions on the following implementation issues: (1) development of a high order AMB parametric model to fit experimental calibration data; (2) design of a look-up-table to implement the feedback linearization algorithm within the digital controller; (3) evaluation and compensation of the influence of the dynamics of AMB system peripheral devices, such as power amplifiers and sensors, on the linearized system; and (4) estimation of the uncertainty and development of a robust controller.

The arrangement of the rest of this paper is as follows. In Section 2, the concept of feedback lin-

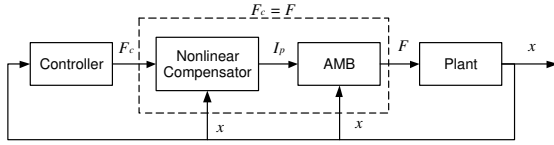


Figure 1: Feedback linearized AMB system.

earization is briefly discussed. Section 3 presents our experimental test rig. Section 4 follows with an examination of AMB modeling and a nonlinear compensation. The influence of the amplifier and sensor dynamics on our system is examined in Section 5. In Section 6, we propose a feedback linearization uncertainty framework, which is then used in a robust controller design procedure in Section 7. Finally, a summary is provided in Section 8.

2 FEEDBACK LINEARIZATION

For a laminated magnetic bearing, its electromagnetic force, f , can be expressed as a static nonlinear function of the controlled coil current, I_p , and the journal displacement from the center position, x :

$$F = f(I_p, x) \quad (1)$$

We can choose the controlled current I_p as the inverse function of Eqn(1) with respect to the displacement x and a reference force F_c

$$I_p = f^{-1}(F_c, x) \quad (2)$$

to cancel the nonlinear function $f(I_p, x)$. Consequently, the system is linearized. Figure 1 shows this feedback linearization in block diagram form.

We can remark that this feedback linearization scheme does not depend on the plant dynamics since the nonlinear electromagnetic force is linearized before affecting the plant's states. The resulting linear system is valid across the entire range of operation. Furthermore, since the system from F_c to x behaves linearly, the control problem on the original nonlinear system is simplified to a linear control problem. Finally, since $F_c = F$, the linear controller can be designed based on the plant dynamics from F to x as if the AMB does not exist.

3 AMB TEST RIG

Figure 2 shows the machining test rig with AMB actuator employed in our study. The test rig consists of two platforms connected by a leaf spring, and constrained to single axis rectilinear motion in the

feed direction by flexures. The tool platform holds a cutting tool and the actuator platform is rigidly connected to the bearing journal, which is made of a cobalt iron laminations. This journal can be driven by the AMB stator which is mounted above the actuator platform. The magnetic bearing stator used is a conventional eight pole radial design. Two groups of coils, driven by two identical 150V *Pulse Width Modulation* (PWM) power amplifiers, generate opposing attractive forces along the feed direction. A bias current of 1A is applied to coils to guarantee sufficient force slew rate for the application. The air gap of the bearing is approximately 250 μm on each side. An eddy current transducer is used as a position sensor to measure the journal motion (hence air gap).

The entire test rig is mounted on a lathe and can be fed into a rotating workpiece to conduct cutting operations. A dSPACE *DS1103* digital control system is applied on the AMB actuator.

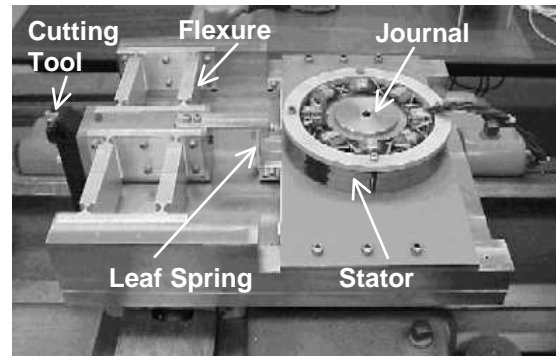


Figure 2: Photograph of the AMB test rig.

4 AMB MODELING

4.1 AMB CALIBRATION

An accurate nonlinear model is necessary for the feedback linearization. Due to the complexity of electromagnetic field, it is difficult to obtain accurate analytical models for AMBs. However, as stated in Eqn (1), the force-current-gap relationship can be established from appropriate experimental tests on the AMB. Therefore, we may avoid the disadvantages of analytical models.

For calibration, we used a stiff spring to pull the actuator platform along (or opposite to) the feed direction. A PID controller was designed to stabilize the actuator platform at any specified air gap. The spring force, air gap, and bearing current were measured by a load cell, eddy current sensor, and current

monitors, respectively. The calibration was carried out in the following manner. With a known spring force applied and a specified position offset on the platform, the PID controller regulated the AMB's current to generate the proper electromagnetic force to balance the external force acting on the platform:

$$F = -F_{spring} - kx \quad (3)$$

where k is the static stiffness of the actuator platform flexures, and F_{spring} is the measured spring force obtained from the load cell. After transients have decayed, the calculated electromagnetic force, the specified air gap, and the corresponding measured input current together are one set of static calibration data. The AMB was calibrated at different positions over the entire clearance, and at different coil current ranging from $-1A$ to $1A$. During the calibration, the AMB was degaussed frequently to reduce the effect of hysteresis. Figure 3 shows the calibration results, which confirms the nonlinearity of the AMB.

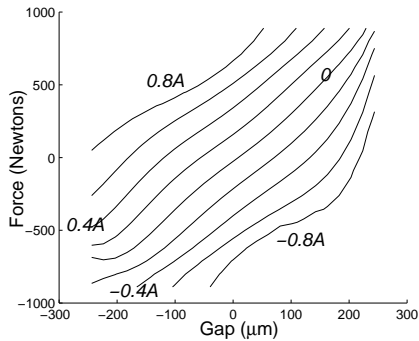


Figure 3: AMB calibration results.

4.2 PARAMETRIC AMB MODEL

Applying the multi-variable Taylor series expansion on Eqn(1) around $I_{p,0} = 0$ and $x_0 = 0$, we can get

$$f(I_p, x) = a_0 + a_1 I_p + a_2 x + a_3 I_p^2 + a_4 I_p x + a_5 x^2 + a_6 I_p^3 + a_7 I_p^2 x + \dots \quad (4)$$

where a_0, a_1, \dots are the coefficients in the Taylor expansion. These values can be determined by a least-squares fit of the calibration results. Note that the traditional Jacobian linearization uses only the first three terms in Eqn(4), while the order of the general nonlinear model may be chosen as desired so as to achieve an accurate representation over the entire operating range.

It was found that inclusion of terms up to 5^{th} order resulted in a highly accurate representation of the data. A comparison of the errors for this model and that of the standard Jacobian linearization is shown in Figure 4.

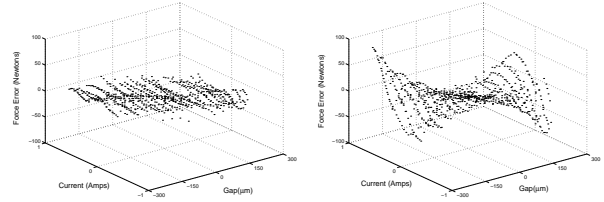


Figure 4: Force errors of the 5^{th} order nonlinear (left) and the Jacobian linear (right) models.

4.3 NONLINEAR COMPENSATOR

For a static feedback linearization, we seek to find a nonlinear compensator that yields AMB current inputs such that the applied electromagnetic force, F , equals the reference force provided to the nonlinear compensator, F_c , at the measured bearing air gap x . Therefore, the proper current, I_p , should be the solution of the equation

$$F_c - f(I_p, x) = 0 \quad (5)$$

Substituting the AMB polynomial model of Eqn(4) into Eqn(5), we can solve for I_p . Although there are multiple solutions due to the high order of the AMB model, the appropriate solution may easily be chosen by satisfying two conditions: $I_p \in \mathbf{R}$ and $|I_p| \leq 1A$ (the bias current).

The linearizing current was calculated for each air gap from $-250\mu m$ to $250\mu m$, with $5\mu m$ increments, and each force from $-1000N$ to $1000N$, with $10N$ increments. Then these results were stored in a 2-D *Look-Up-Table* (LUT). For inputs not in the table, the LUT uses either interpolating or extrapolating techniques to perform linear mapping from inputs F_c and x to output I_p . Compared to the traditional inverse function computation methods, LUT has better computational efficiency, and is easier to implement in the dSPACE digital controllers.

5 EFFECT OF SYSTEM DYNAMICS

Ideally the LUT generates the proper current to cancel the AMB nonlinearity independent of the frequency of the desired force signal. Nevertheless, in practice, the position input signal to the LUT is not dynamically equivalent to the actual signal due to the dynamics of the devices conducting the

measurement. The air gap signal is colored by the eddy current sensor and anti-aliasing filter dynamics. Furthermore, the current signal commanded by the LUT is not equivalent to the actual coil current signal. Rather, the later is a colored version of the command signal due to the PWM and D/A converter dynamics. These dynamics increase the error of the cancellation in the system, and degrade the feedback linearization performance.

In order to attenuate this problem, high bandwidth sensors and amplifiers should be used in the system. However, even with good devices, it may be necessary to employ carefully designed corrective filters, connected in series with these devices, to compensate their dynamics. These filters should make the input/output signals of LUT very close to the corresponding signals in AMB, over the control bandwidth of the system.

An alternative approach to feedback linearization of this system would be to include these dynamics into the feedback linearization itself (i.e., a dynamics feedback linearization as opposed to the static approach taken here - see [3] for example). However, the authors believe that this more technically rigorous approach would prove to be very difficult to carry out considering the complexity of the actuator dynamic behavior.

Figure 5 shows the feedback linearized system diagram with two digital filters. Filter *I* is used to compensate for the dynamics of the eddy current sensor, anti-aliasing filter, and A/D converter. Filter *II* is used to compensate for the dynamics of the D/A converter and PWM amplifiers. These filters were designed based on the open loop frequency responses of these two signal paths. Figure 6 shows the frequency responses before and after using these two filters. The comparison shows that both magnitude variations and phase lag of the signal paths were reduced by using these filters.

One method to verify the effectiveness of this compensation is to examine the frequency response of the feedback linearized system. If perfect linearization was achieved, the linearized system's frequency response from reference input F_c (as shown in Fig-

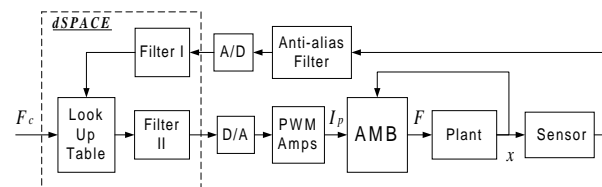


Figure 5: Filtered system diagram.

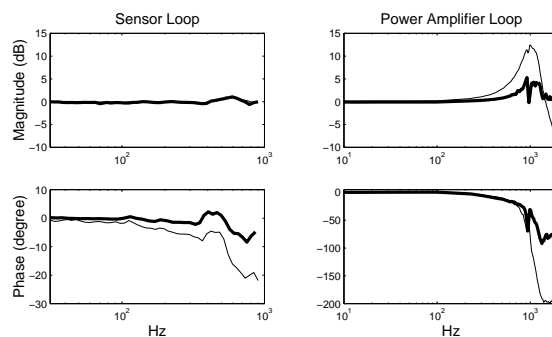


Figure 6: Frequency responses comparison for sensor and amplifier signal paths before compensation (thin line) and after compensation (thick line).

ure 5) to plant output x , $G_{pfl}(j\omega)$, would be equal to the open loop plant frequency response from F to x , $G_p(j\omega)$. To evaluate this, impact tests were performed. A comparison of measured $G_{pfl}(j\omega)$ with and without the filter compensation along with the measured $G_p(j\omega)$ is shown in Figure 7. It is clear that the compensation has greatly improved the quality of the feedback linearization.

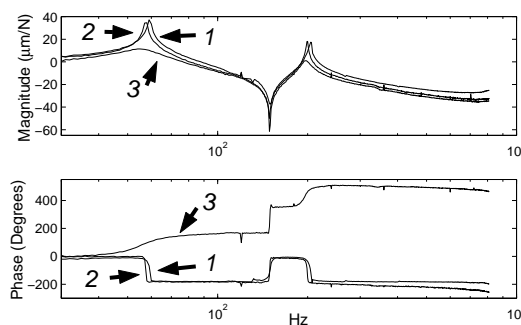


Figure 7: Open loop frequency response comparison. Curve 1: open loop plant frequency response $G_p(j\omega)$; Curve 2/3: open loop frequency response $G_{pfl}(j\omega)$, after/before using filters.

6 UNCERTAINTY REPRESENTATION

Feedback linearization renders the nonlinear AMB and amplifier as essentially a static gain. Therefore, we can employ the actuator platform's model as the nominal model of the whole feedback linearized system. Since both the AMB and nonlinear compensator depend on the feedback of the platform displacement, we have developed a displacement feedback uncertainty structure, to represent the remaining mismatch between this nominal model and the linearized systems behavior. Figure 8 shows the

structure, where the uncertainty is defined as

$$\Delta_c := \frac{G_{pfl}(j\omega) - G_p(j\omega)}{G_{pfl}(j\omega) \cdot G_p(j\omega)} \quad (6)$$

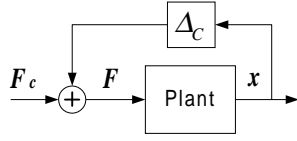


Figure 8: Complex uncertainty representation.

Experimental validations were conducted to estimate the magnitude of this uncertainty. First, the position of the platform was regulated by a PID controller. Then, frequency responses of $G_{pfl}(j\omega)$ and $G_p(j\omega)$ were measured at that position through impact tests. The differences between these two frequency responses were calculated by Eqn (6) at measured frequencies. Furthermore, in order to evaluate the uncertainty over the entire operating range, more frequency responses were measured at various positions. The magnitude of the uncertainty set can be determined by finding the smallest circle in the complex plane to enclose almost all of the resulting data points. Figure 9 shows the boundary of our feedback linearization uncertainty, which is estimated from approximately 2500 solutions.

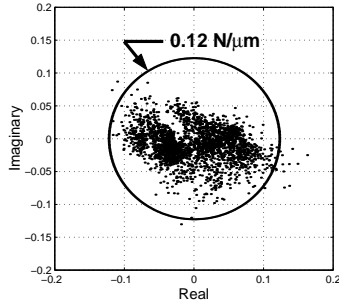


Figure 9: Uncertainty estimation.

7 ROBUST CONTROLLER DESIGN

μ synthesis offers a systematic framework for the design of controllers that meet H_∞ performance objectives and guarantee robustness to structured model uncertainty. Figure 10 shows the experiment block diagram with its uncertainty structure, where the tool platform and actuator platform blocks contain their corresponding nominal models; K_s is the stiffness of the leaf spring; F_M and x_T are the cutting

force input and tool's displacement, respectively; Δ_1 is the unit norm-bounded feedback linearization uncertainty, and W_1 is its weight (i.e., $\Delta_c = W_1\Delta_1$).

The control goal is to increase machining stability by minimizing the tool compliance from F_M to x_T , with a reasonable control effort. There are two fictional complex uncertainties, Δ_2 and Δ_3 , in the synthesis framework, and their associated weights, W_2 and W_3 , can be used to specify the system's performance goals. If $\mu < 1$ is achieved in synthesis, then the controller will achieve a tool compliance less than $\|W_2(j\omega)^{-1}\|$ at each frequency, and the controller gain will be approximately constrained by $\|W_3(j\omega)^{-1}\|$.

A μ controller was designed by D-K iterations using MATLAB μ toolbox. The resulting controller was 18th order, and was reduced to 6th order via a balance-and-truncate algorithm without a notable loss of robustness or performance. For evaluation purpose, we have introduced a position offset x_0 to adjust the bearing air gap, as shown in Figure 10. An integral term $-50/s$ was connected in parallel with the μ controller to improve the static performance of tracking x_0 . The controller was implemented on the dSPACE digital controller with a sampling rate of 20 kHz.

In order to verify the effectiveness of the feedback linearization over the entire clearance, seven journal locations from $-180\mu\text{m}$ to $180\mu\text{m}$ from center, with an increment of $60\mu\text{m}$, were specified by the offset signal. The closed loop tool compliances were measured at each location and these are compared with the open loop compliance in the left plot of Figure 11. The open loop structure has a lightly damped resonance frequency at 65Hz, while the closed loop tool is well damped. The plot shows that the variation in the frequency response at different locations is very small, and the closed loop compliance in each case is below W_2^{-1} at all frequencies, as specified. Therefore, the robust performance goal is achieved. To see the importance of the dynamics compensa-

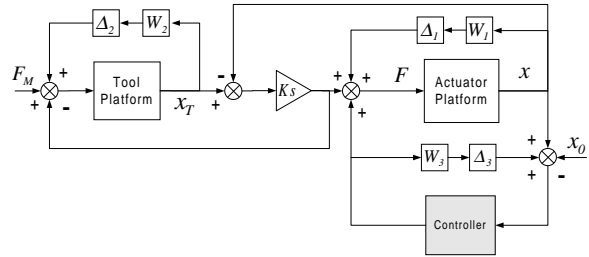


Figure 10: Nominal linearized system with uncertainty and performance weights.

tion filters in the feedback linearization, the closed loop tool compliance at the center position of the bearing was also measured after removing both filters in the system. Its response is shown in the right plot of Figure 11, and compared with the response where the filters are employed. As can be seen, the compensation filters are essential to meeting performance goal.

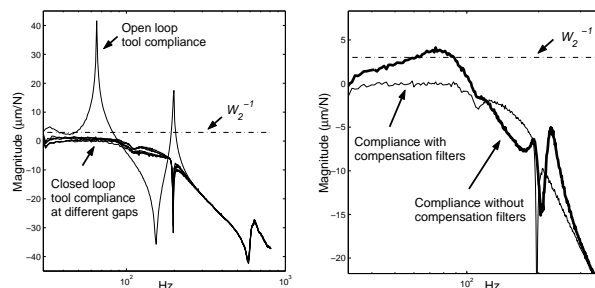


Figure 11: Tool compliance frequency response.

While the frequency responses from impact tests verify the system's small input responses at different locations, it is also interesting to see the system's response under a larger input. Therefore, we applied a band limited white noise input as x_0 , and measured the time response of the journal's displacement. We also put the same input into the nominal linear system (as shown in Figure 10 without the uncertainty blocks). Figure 12 shows the measured response along with the calculated response of the linear model. It can be seen that the experimental response closely matches that of the closed loop linear system over large displacements.

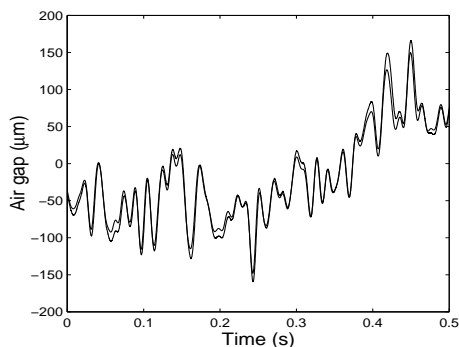


Figure 12: Linear model vs. experimental journal displacement when excited by band limited noise.

8 SUMMARY

A feedback linearization approach has been developed using experimental data and implemented on

an AMB test rig. Experimental data are used to develop a look-up-table to invert the actuator's current-force relation. Filters are introduced to compensate the input and output signal of the look-up-table so as to render the feedback linearized system as nearly equivalent to the open loop model in spite of the dynamics of the A/D, D/A, amplifiers, anti-aliasing filter, and position sensor. Finally a robust control framework for the feedback linearized system was proposed. Experimental results demonstrated that both robust performance and long range stable movement can be achieved under this feedback control.

REFERENCES

- [1] Trumper, D., 1997, "Linearizing Control of Magnetic Suspension Systems", *IEEE Trans. on Contr. Sys. Tech.*, 5(4), pp.427-437.
- [2] Kim, C. Y. and Kim, K. H., 1994, "Gain Scheduled Control of Magnetic Suspension systems", *Proc. American Control Conf.*, pp. 3127-3131.
- [3] Lindlau, J. and Knospe, C., 2002, "Feedback Linearization of an Active Magnetic Bearing with Voltage Control", *IEEE Trans. on Cont. Sys. Tech.*, 10(1), pp.21-31.
- [4] Gutierrez, H. and Ro, P., 1998, "Parametric Modeling and Control of a Long-Range Actuator Using Magnetic Servo Levitation", *IEEE Trans. on Magnetics*, 34(5), pp.3689-3695.
- [5] Joo, S. and Seo, J., 1997, "Design and Analysis of the Nonlinear Feedback Linearizing Control for an Electromagnetic Suspension System", *IEEE Trans. on Cont. Sys. Tech.*, 5(1), pp.135-143.
- [6] Silva, I., 2000, "An Attraction-Type Magnetic Bearing with Control in a Single Direction", *IEEE Trans. on Industry Applications*, 36(4), pp.1138-1142.
- [7] Schroder, P., 2001, "On-Line Evolution of Robust Control Systems: An Industrial Active Magnetic Bearing Application", *Control Engineering Practice*, 9, pp.37-49.
- [8] Lin, L., and Gau, T., 1997, "Feedback Linearization and Fuzzy Control for Conical Magnetic Bearings", *IEEE Trans. on Cont. Sys. Tech.*, 5(4), pp.417-426.
- [9] Minihan, T., 2003, "Large Motion Tracking Control for Thrust Magnetic Bearings with Fuzzy Logic, Sliding Mode, and Direct Linearization", *Journal of Sound and Vibration*, 263, pp.549-567.
- [10] Jeng, J., 2000, "Nonlinear Adaptive Inverse Control for the Magnetic Bearing System", *Journal of Magnetism and Magnetic Materials*, 209, pp.186-188.